Modern Physics Letters B, Vol. 8, Nos. 8 & 9 (1994) 491–503
© World Scientific Publishing Company

(18)

SURFACE MELTING AND SURFACE ROUGHENING OF Pb(110) STUDIED BY LOW ENERGY ION SCATTERING

S. SPELLER, M. SCHLEBERGER, H. FRANKE, C. MÜLLER, and W. HEILAND
Universität Osnabrück, Fachbereich Physik, D-49069 Osnabrück, Germany

Received 11 March 1994

The Pb(110) surface undergoes two phase transitions. At about 400 K a roughening transition is observed. At 580 K, i.e. about 20 K below the bulk melting point, surface melting is found. The surface develops point defects at rather low temperatures. The roughening is connected with the generation of steps or the reduction of terrace size. There is also evidence for anisotropy of the roughening transition. Low energy ion scattering experiments in the temperature range from 160 to 590 K are used to study the structural changes of the Pb(110) surface.

1. Introduction

The Pb(110) surface has been studied in great detail with any possible surface sensitive experimental technique and theoretical models.[1–3] The interest on this particular surface is related to the more general phenomena of surface phase transitions, i.e. surface roughening and surface melting. Roughening effects have been observed on a number of fcc(110) surfaces. Surface melting is experimentally proven on Pb(110)[1,4,5] and Al(110).[1,6] The roughening effect is disputed in some cases, e.g. Pd(110).[7,8] An order–disorder transition was reported to occur on Pd(110) at 250 K,[7] an effect not found in other studies.[8] On Pb(110) and Al(110) the effect is well established. On other fcc(110) surfaces, e.g. Au(110), Pt(110), and Ir(110), the roughening transition is coupled to a 2D surface phase transition. The state of the art is summarized in Table 1.[9–34] The tables summarizes results for fcc(110) without a structural phase transition (part a) and with an order–disorder transition (part b). Since roughening is defined as the divergence of the height–height correlation function it is more clearly measured by diffraction techniques. In real space experimental techniques the number of steps which increases at some temperature is used as the signature of roughening. But in diffraction techniques also the number of steps is an accessible parameter, so we find also with diffraction techniques roughening characterized by step numbers. Another point of confusion is the observation of anharmonic or enhanced thermal vibrational amplitudes of surface atoms; these amplitudes can be misinterpreted as the signature of roughening. Cu(110) has a record of this kind. The early finding of photoelectron spectroscopy that

Table 1. Surface roughening of fcc(110) surfaces. (a) Without phase transition. (b) With phase transition.

		T_R(K)	T_R/T_M	T_M(K)	Method	Reference
(a)	Ag(110)	720 ± 25	0.58	1233	X-rays	G. A. Held *et al.*[9]
		992	0.80		X-rays	I. K. Robinson *et al.*[10]
		910 ± 15	0.75		HEAD	G. Bracco *et al.*[11]
	Al(110)	620	0.70	933	LEED	P. von Blankenhagen[12]
		753 ± 10	0.80		LEED	A. Pavlovska *et al.*[13]
		770 ± 25	0.82		X-rays	H. Dosch *et al.*[14]
		815	0.87		MEIS	A. W. D. van der Gon *et al.*[6,15]
	Cu(110)	870	0.64	1356	X-rays	S. G. J. Mochrie[16]
		870	0.64		IPES, LEIS	R. Schneider *et al.*[17]
						Th. Fauster *et al.*[18]
		1070	0.79		HEAD	P. Zeppenfeld *et al.*[19]
						K. Kern[20]
	In(110)	290	0.69	430	Crystal shaped	J. C. Heyraud *et al.*[21]
						A. Pavlovska *et al.*[22]
	Ni(110)	1270	0.74	1726	LEED	Y. Cao *et al.*[23]
	Pb(110)	415	0.69	600	LEED	H. N. Yang *et al.*[24]
		400 ± 10	0.67		XPD	H. P. Bonzel *et al.*[25]
					LEED	U. Breuer *et al.*[26]
		420	0.70		LEED	A. Pavlovska *et al.*[22,27]
		500	0.83		MEIS	A. W. D. van der Gon *et al.*[28]
		390 ± 10	0.65		LEIS	This work
(b)	Au(110)	650 ± 20	0.49	1336	LEIS	E. van de Riet *et al.*[29]
		690	0.52		HEAD	J. Sprösser *et al.*[30]
	Ir(110)	1055 ± 20	0.40	2680	LEIS	W. Hetterich *et al.*[31]
	Pt(110)	1080	0.53	2042	X-rays	I. K. Robinson *et al.*[32]
		900 ± 20	0.44		RHEED	U. Korte *et al.*[33]
		1030 ± 25	0.50		FEM	R. Vanselov[34]

T_R — roughening temperature, T_M — bulk melting temperature
LEED — Low Energy Electron Diffraction
MEIS — Medium Energy Ion Scattering
IPES — Inverse Photo-Electron Spectroscopy
LEIS — Low Energy Ion Scattering
XPD — X-ray Photoelectron Diffraction
HEAD — HE Atom Diffraction
RHEED — Reflection High Energy Electron Diffraction
FEM — Field Electron Microscopy

the spectra at 800°C were equivalent to polycristalline Cu was interpreted as thermal disorder.[35] Later numerous steps were found at 600°C.[16] No roughening was reported up to 900 K from HEAD experiments.[19] Later roughening was found by the same techniques at 1070 K.[20] The LEIS results of Ref. 19 were partly discussed as being due to anharmonic thermal vibrations.[36] The theory predicts in general roughening transition temperatures of about $T_R = 0.7\ T_M$, where T_M is the bulk melting temperature. Surface melting is theoretically discussed within molecular dynamics calculations[3] and thermodynamics.[37] So far the theory makes no quantitative prediction with respect to surface melting beside the facts that when surface melting occurs, certain dependencies should be observed, e.g., logarithmic growth of the molten surface layer thickness with temperature. In the following we will report results of low energy ion scattering experiments which give additional evidence of surface roughening and surface melting on Pb(110). Some results have been published previously.[6,38–39] These will be summarised shortly and discussed together with new data.

2. Experiment

The experimental data are collected using the techniques of low energy ion scattering, i.e. surface channeling, neutral impact collision ion scattering spectrometry (NICISS), and plain ion yield measurements.[40] The experimental setup provides a mass analyzed ion beam from 100 eV to 10 keV. Here we use 2 keV Ne for the surface channeling and the NICISS. The surface channeling uses two modes, i.e. forward scattering of the incident ions with measurements of the channeling patterns using a position sensitive detector.[41] This mode is true surface channeling[42] as long as the (grazing) angle of incidence is kept small enough such that total particle reflection is obtained.[43] For the second mode of operation we use a time of flight (TOF) system. The primary beam is pulsed and a channeltron is located at a scattering angle of 165° for the detection of backscattered neutrals. We keep the impact angle fixed and vary the azimuthal angle. By this means the periodicity of the surface is monitored in real space.[44] Structural phase transitions are easily monitored as well as qualitative information about steps on the surface. When using the TOF system in the NICISS mode the azimuthal angle is fixed and the angle of incidence is varied. This type of experiment uses the shadow cone effect in order to measure surface lattice constants. For ion yield measurements an electrostatic analyser (90° spherical) is used. Further experimental details have been published previously.[45,46] The system provides also a LEED setup for probing the periodicity of the surface in reciprocal space. Good surface channeling patterns are clearly correlated to good LEED patterns. The quantitative evaluation of the channeling patterns is comparably simple because classical ion scattering codes can be used in our range of ion energies whereas LEED needs detailed I–V curve analysis and a "dynamical" code.

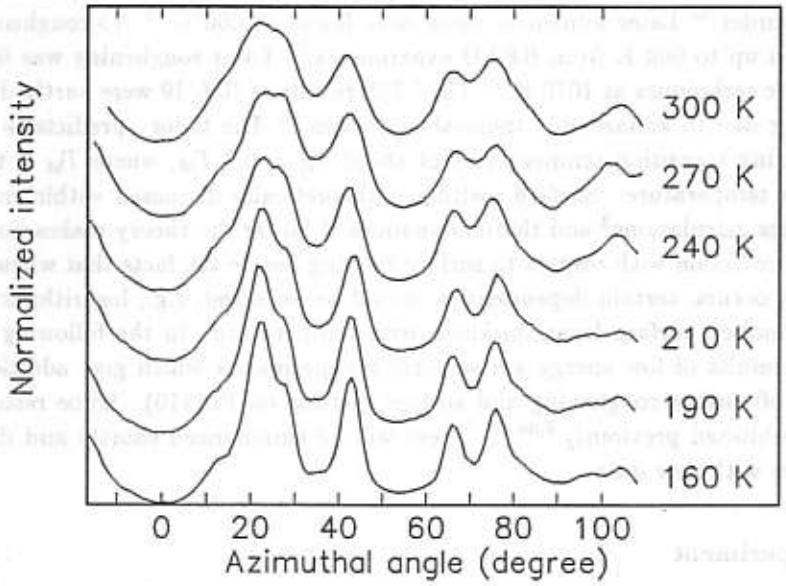

Fig. 1. Temperature dependence of the 'blocking' patterns from a Pb(110) surface. The patterns are obtained using a 2 keV Ne beam at grazing incidence and detecting the backscattered neutrals at a scattering angle of 165°. The parameter varied is the azimuthal angle. The minimum at 0° is the $\langle 1\bar{1}0 \rangle$ surface direction and at 90° is the $\langle 001 \rangle$ direction.

3. Results

In the first part we will present results in the low temperature regime from about 160 K to room temperature. Figure 1 shows surface channeling results in the backscattering or blocking mode between 160 and 300 K over a range of the azimuthal angle of 120 degrees. This is sufficient to cover the crystal surface structure from the $\langle 1\bar{1}0 \rangle$ to the $\langle 001 \rangle$ surface direction. Other low index directions clearly resolved as intensity minima in this mode of ion scattering are the $\langle 1\bar{1}1 \rangle$, $\langle 1\bar{1}2 \rangle$ and $\langle 1\bar{1}4 \rangle$ surface directions. The minimum yields are a qualitative measure of the step density of the surface. Here the yields are higher in comparison with, e.g., Au(110) or Pt(110) which are known to form rather large terraces when prepared carefully.[33,47] More information about steps can be obtained when using the NICISS mode which also provides information about the surface lattice parameters and surface point defects (Table 2).[5] We added here the analysis of the first to second layer distance. The surface is contracted and the contraction is in the temperature range reported here independent from the temperature. The number of surface point defects also depends little on temperature. The surface thermal vibrational amplitudes follow a Debye behavior. We find an expansion of the $\langle 110 \rangle$ surface atom distance of up to 10% which is larger than the normal bulk thermal expansion. Furthermore, this expansion is anisotropic, i.e. there is no effect in the $\langle 1\bar{1}2 \rangle$ direction.

Table 2. The root mean square thermal amplitude perpendicular to the surface $[(\Delta z)^2]^{1/2}$, the critical impact angle Ψ_c, the surface lattice constant a, the relative number of vacancies n in the two top layer $[1\bar{1}0]$ chains, the mean square displacement q between the experimental and the calculated I vs Ψ distributions for three temperatures, and d_{12}, the layer spacing (contraction) between the first and second layer relative to the bulk spacing.

	T(K)		
	160	276	395
$[(\Delta z)^2]^{1/2}$ (Å)	0.207	0.271	0.324
Ψ_c, $[1\bar{1}0]$ (deg)	22.70	22.06	21.18
Ψ_c, $[1\bar{1}2]$ (deg)	14.66	14.66	14.66
a $[1\bar{1}2]$ (Å)	6.06	6.06	6.06
a $[1\bar{1}0]$ (Å)	3.50 ± 0.01	3.63 ± 0.01	3.82 ± 0.01
n $[1\bar{1}0]$ (%)	10.4 ± 2	8.8 ± 2	9.2 ± 2
n $[1\bar{1}2]$ (%)	10.3 ± 2	9.2 ± 3	13.6 ± 4
q $[1\bar{1}0]$ (10^{-5})	6.1	3.2	3.8
q $[1\bar{1}2]$ (10^{-4})	6.2	3.2	2.5
d_{12} (%)	-19 ± 1.5	-20 ± 1.5	

This is possible if the point defects are randomly distributed over the surface, which is safe to assume. Since we use NICISS, the data are an average over two layers for the $\langle 1\bar{1}0 \rangle$ direction whereas for the $\langle 1\bar{1}2 \rangle$ direction the second layer is 'blocked' as long as the surface is well ordered. The agreement of the number of defects for the two directions indicates that the majority of point defects is in the top surface layer. In Fig. 2 we show the patterns for the forward surface channeling experiment for the $\langle 1\bar{1}0 \rangle$, $\langle 1\bar{1}2 \rangle$, and a high index or 'random' direction at room temperature. These patterns are 'mirror images' of the elastic scattering potential formed by the surface atoms. The random case is almost isotropic, i.e. the surface potential is planar and we have the case of planar semichanneling. For the low index directions we obtain the 'image' of the corrugation of the surface potential due to the conservation of perpendicular momentum of the particles during channeling. The width of the patterns is different due to the different widths of the troughs formed along $\langle 1\bar{1}0 \rangle$ and $\langle 1\bar{1}2 \rangle$ as seen in the blocking mode in Fig. 1. These patterns are not very sensitive to point defects but to steps on the surface which block the troughs. The trajectory lengths are of the order of 10 lattice constants, i.e. terrace widths of the order of 30 Å may be sufficient to produce these patterns. These findings are based on MARLOWE calculations.[44]

If the temperature of the crystal is raised further we observe major changes of the channeling patterns for the low index directions. All directions change into 'random'-like patterns at distinct temperatures. Figure 3 shows the effect as a plot of the shape of the channeling pattern vs temperature for $\langle 1\bar{1}0 \rangle$ and $\langle 1\bar{1}2 \rangle$. The shape is expressed as the aspect ratio of the pattern, i.e. height/width or spatial extension

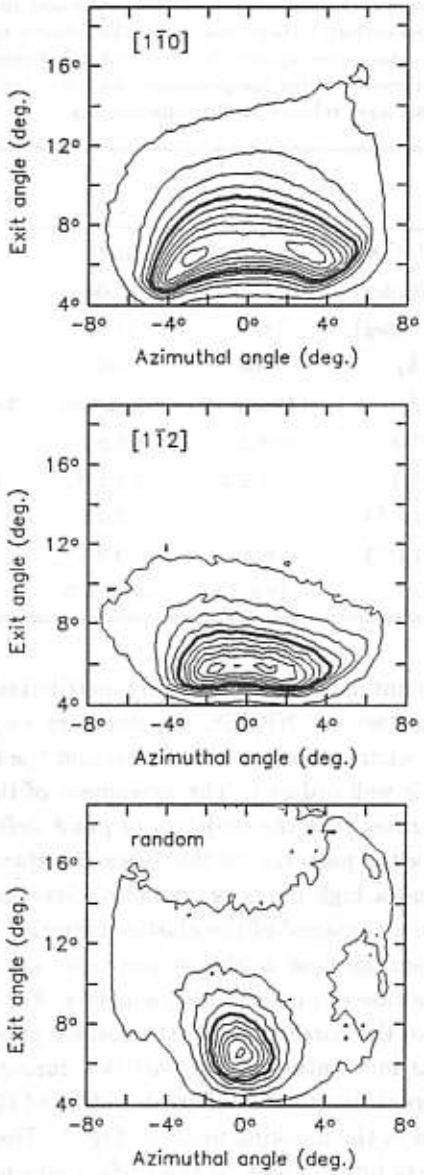

Fig. 2. Surface channeling patterns of Pb(110) for the (a) ⟨1$\bar{1}$0⟩ and (b) ⟨1$\bar{1}$2⟩ surface directions at room temperature. The patterns are measured using a 2 keV Ne beam at grazing incidence and detecting all forward scattered particles using a position sensitive detector. The solid line marks the intensity at FWHM.

in the direction perpendicular to the surface with respect to the width parallel to the surface. Naturally an isotropic pattern yields the shape 1.0. A new result is the obvious anisotropy of the temperature dependence of the structural changes

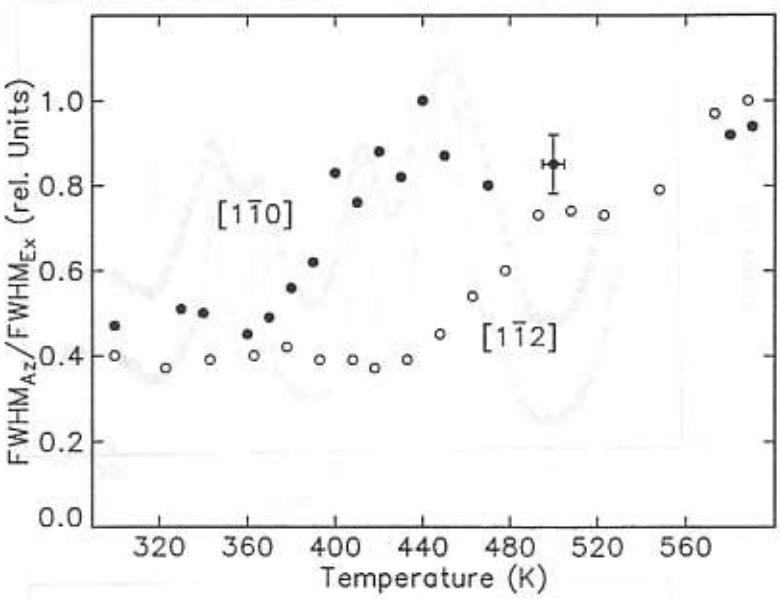

Fig. 3. Temperature dependence of the surface channeling patterns of Pb(110) for the $\langle 1\bar{1}0\rangle$ and $\langle 1\bar{1}2\rangle$ directions expressed by the aspect ratio of the pattern, i.e. the FWHM in the direction perpendicular to the surface/FWHM in the azimuthal direction.

of the surface. The difference between the $\langle 1\bar{1}0\rangle$ and $\langle 1\bar{1}2\rangle$ directions amounts to 70 K. The obvious interpretations for this finding are the differences of the free energies and the differences of the activation energies for step formation and step decay, respectively.[37] For these reasons the low index steps are formed at lower temperatures, here $\langle 001\rangle$ steps which block the channeling along the $\langle 1\bar{1}0\rangle$ direction, compared to higher index steps which are needed to block the $\langle 1\bar{1}2\rangle$ channeling. Previous results gave mere hints for this type of anisotropy[25] or at somewhat higher temperatures, i.e. 500 K, closer to the surface melting point of 580 K.[28] So the disorder seen by MEIS may not be the roughening observed by LEED[24,26,27] and XPD,[25] and by LEIS in this work.

An interesting insight into the roughening gives the comparison of the azimuthal blocking patterns of Au(110) and Pb(110) at 700 K and 420 K, respectively (Fig. 4). The roughening in combination with the order–disorder transition of Au(110) is well established.[29,30] Au(110) at 700 K is a disordered, rough fcc(110) surface and we use it here as a "standard" for the Pb(110) surface. The agreement between the experimental data of the two surfaces is rather astonishing. For comparison we show also the resp. low temperature azimuthal patterns. These are significantly different owing to the (1 × 2) reconstruction of the Au(110) surface. Small differences are due to the difference in the lattice spacing of the $\langle 1\bar{1}0\rangle$ direction of Pb and Au of 2.92 Å and 3.50 Å, respectively, which makes the high index channels wider in the case of Pb. Raising the temperature of Pb(110) under the experimental conditions

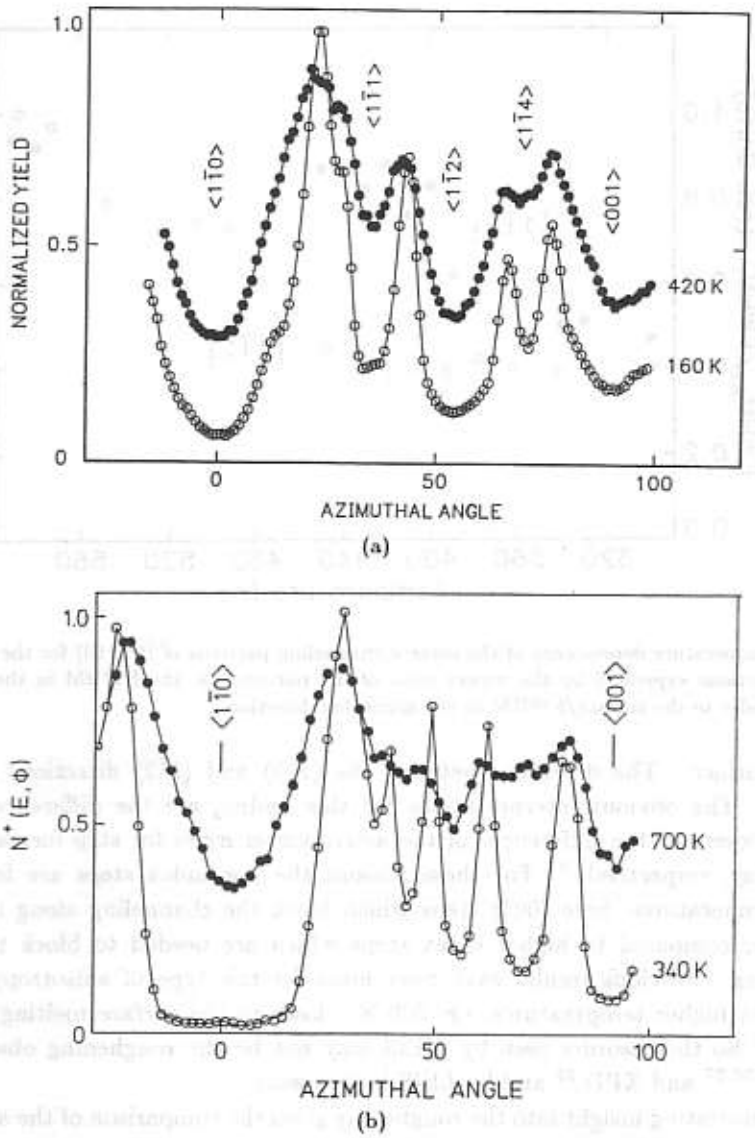

Fig. 4. Comparison of the 'blocking' patterns of (a) Pb(110) and (b) Au(110). The patterns for Pb are at 160 K for a 'well-ordered' surface and at 420 K for a 'rough' surface. The patterns for Au are at room temperature 'ordered (1 × 2)' and at 700 K 'disordered, rough (1 × 1).'

of Fig. 4 cause all azimuthal dependencies to vanish, the curve being simply a straight line.[5] This was the independent confirmation of the surface melting first observed by MEIS.[4] With He as primary ions at similar scattering conditions we find penetration into deeper layers. As a minimum in the azimuthal yield dependence the $\langle 1\bar{1}2\rangle$ direction is pronounced because along this direction the bulk channels are completely open. In principle this observation could be used to gauge the thickness

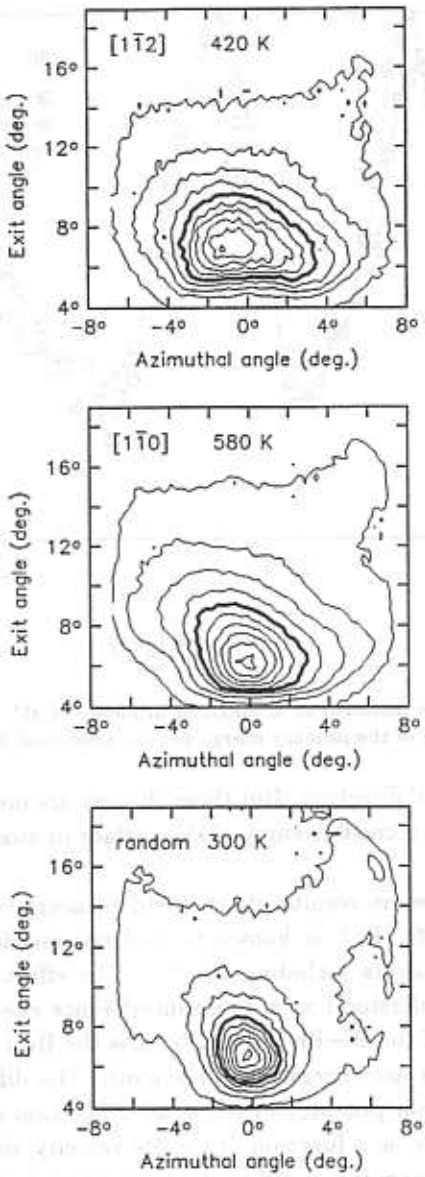

Fig. 5. Surface channeling patterns of Pb(110) at 420 and 580 K for the ⟨110⟩ direction in comparison with a room temperature high index, 'random' pattern.

of the molten layer on top of the bulk crystal as was done by MEIS.[1] Here without detailed trajectory calculations we can only state that a "thin" layer of quasiliquid structure is covering an "ordered" bulk crystal. Using the position sensitive detector in the channeling mode we find some additional "rounding" between 420 and 580 K (Fig. 5). The 580 K pattern shown is very similar to the obtained for scattering along

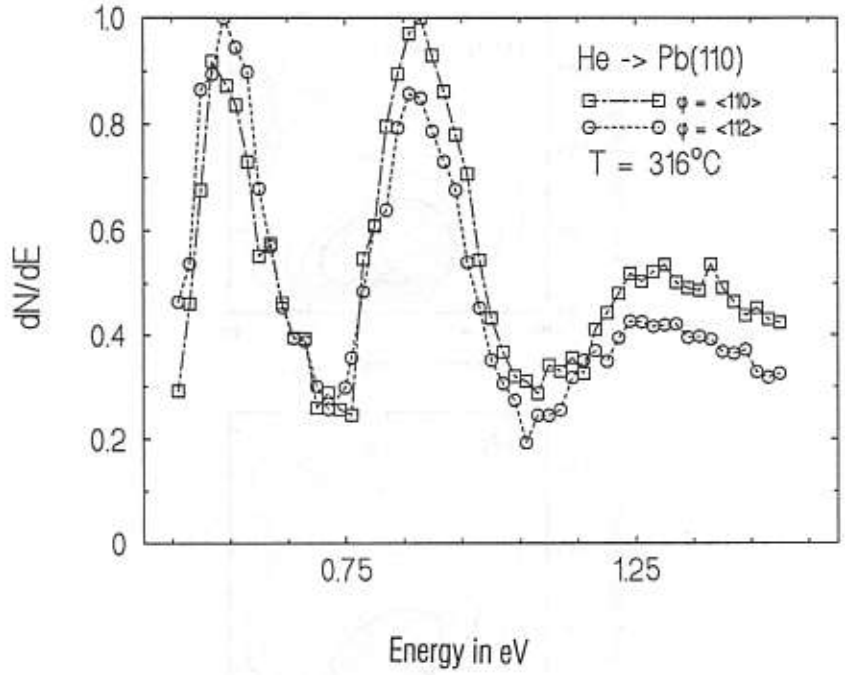

Fig. 6. Ion yield of He ions scattered at an angle of incidence of 45° in a scattering angle of 90° from Pb(110) as a function of the primary energy for two azimuthal directions: $\langle 1\bar{1}0\rangle$ and $\langle 1\bar{1}2\rangle$.

a high index or 'random' direction. But these changes are no further proof of surface melting. They indicate some flattening of the surface in qualitative agreement with all previous results.

Finally we report some results of ion yield measurements of He^+ scattering from Pb(110) in Fig. 6. He^+ is known to undergo quasiresonant neutralisation with a number of elements including Pb.[48,49] The effect, named "Stueckelberg oscillations",[50,51] is understood as a phase interference effect of the electron wave function. In the case of the He–Pb interaction it is the He 1*s* state interacting with the Pb 5*d* states which are energetically resonant. The difference of the He^+–Pb and He^0–Pb^+ interaction potentials causes, as a function of the distance of closest approach, and hence as a function of the He velocity, different "path lengths". Therefore the particle acquires a different phase which is then causing the interference effect at the exit of the mixing region of the wave function. At room temperature we find an azimuthal dependence of the amplitudes of the ion yield as a function of the He ion energy.[52,53] For the closed-packed $\langle 1\bar{1}0\rangle$ direction the peak intensities at 0.54 eV and 0.88 keV have a ratio of 1.54, whereas for the $\langle 1\bar{1}2\rangle$ direction the intensity ratio is 1.28 at room temperature. In the quasiliquid phase the peak intensity ratio is 1.0 for both directions within the experimental scatter of the data (Fig. 6). Since the frequency of the oscillations is not changing we

can exclude all the mechanisms which would invoke a change of either the 1*s* He state or the 5*d* Pb states with temperature. The intensity maxima of the ion yield curves represents the Auger neutralisation part of the ion surface interaction.[51,53] The Auger neutralisation is *per se* not temperature dependent.[54] The neutralisation depends, however, on the trajectory length or on the number of atoms the ion passes over during the interaction,[55–59] i.e. the neutralisation becomes azimuthally dependent by virtue of the interatomic distances of the atoms along a given surface direction. In the example studied here the He ions "sample" more electrons at the Fermi edge when they scatter along the closed-packed directions, $\langle 1\bar{1}0\rangle$, compared to the rather open $\langle 1\bar{1}2\rangle$ directions. In the temperature region of surface melting the average distance between the surface atoms should be randomized, hence no azimuthal dependence is observed (Fig. 6).

4. Summary

In this report we summarised the known data on fcc(110) surfaces which show the effect of surface roughening (Table 1). To a greater detail we summarised our data of LEIS experiments on the Pb(110) surface including the surface melting effect. The roughening is clearly demonstrated using a surface channeling technique. The data also give evidence for an anisotropy related to the step structure of the surface. The azimuthal blocking pattern technique confirms the surface melting effect. The same technique in a comparison of Pb(110) data with Au(110) data shows that the two surfaces form an almost identical rough, disordered surface phase at 420 and 700 K, respectively. Measurements making extensive use of the shadow cone effect (Table 2) give evidence for vacancy formation in the top surface layers, and for an anomalous anisotropic lattice expansion effect. The same technique has been used to measure the mean amplitudes of the thermal surface atom vibrations. They follow the high temperature approximation of the Debye theory. The distance between the first and second layer was also measured. The distance between the top planes is contracted by 20% ± 2% compared to the bulk distance, in agreement with previous MEIS results.[1] The contraction decreases slightly with increasing temperature.

Acknowledgements

This work is supported by the Deutsche Forschungsgemeinschaft (DFG). We thank A. Pavlovska (Clausthal) for sending the In data[22] prior to publication.

References

1. J. F. van der Veen, in *Phase Transitions in Surface Films, NATO ASI Series*, eds. H. Traub *et al.* (Plenum, New York, 1991) p. 289.
2. E. H. Conrad and T. Engel, *Surf. Sci.* **299–300**, 391 (1994).
3. M. Bernasconi and E. Tosatti, *Surf. Sci. Repts.* **17**, 363 (1993).
4. J. W. M. Frenken and J. F. van der Veen, *Phys. Rev. Lett.* **54**, 134 (1985).

5. S. Speller, M. Schleberger, A. Niehof, and W. Heiland, *Phys. Rev. Lett.* **68**, 3452 (1992).
6. A. W. D. van der Gon, B. Pluis, R. J. Smith, and J. F. van der Veen, *Surf. Sci.* **209**, 431 (1989).
7. S. M. Francis and N. V. Richardson, *Phys. Rev.* **B33**, 662 (1986).
8. A. M. Lahee, J. P. Toennies, and Ch. Wöll, *Surf. Sci.* **191**, 529 (1987).
9. G. A. Held, J. L. Jordan-Sweet, P. M. Horn, A. Mak, and R. J. Birgenau, *Phys. Rev. Lett.* **59**, 2075 (1987).
10. I. K. Robinson, E. Vlieg, H. Hörnis, and E. H. Conrad, *Phys. Rev. Lett.* **67**, 1890 (1991).
11. G. Bracco, C. Malò, C. J. Moses, and R. Tatarek, *Surf. Sci.* **287–288**, 871 (1993).
12. P. von Blankenhagen, W. Schommers, and V. Voegel, *J. Vac. Sci. Tech.* **A5**, 649 (1987).
13. A. Pavlovska, M. Tikhov, Yingjun Gu, and E. Bauer, *Surf. Sci.* **221**, 233 (1989).
14. H. Dosch, T. Höfer, J. Peisl, and R. L. Johnson, *Europhys. Lett.* **15**, 527 (1991).
15. A. W. D. van der Gon, R. J. Smith, J. M. Gay, D. J. O'Connor, and J. F. van der Veen, *Surf. Sci.* **227**, 143 (1990).
16. S. G. J. Mochrie, *Phys. Rev. Lett.* **59**, 304 (1987).
17. R. Schneider, H. Dürr, Th. Fauster, and V. Dose, *Vacuum* **41**, 528 (1990).
18. Th. Fauster, R. Schneider, H. Dürr, G. Engelmann, and E. Taglauer, *Surf. Sci.* **189–190**, 610 (1987).
19. P. Zeppenfeld, K. Kern, R. David, and G. Comsa, *Phys. Rev. Lett.* **62**, 63 (1989).
20. K. Kern, *Surface Science — Principles and Applications*, eds. R. F. Hove, R. N. Lamb, and K. Wandelt, *Springer Proc. Phys.* **73**, 81 (1993).
21. J. C. Heyraud and J. J. Metois, *J. Cryst. Growth* **82**, 269 (1987).
22. A. Pavlovska and E. Bauer, private communication.
23. Y. Cao and E. H. Conrad, *Phys. Rev. Lett.* **64**, 447 (1990).
24. H. N. Yang, T. M. Lu, and G. C. Wang, *Phys. Rev. Lett.* **63**, 1621 (1989).
25. H. P. Bonzel, U. Breuer, and M. Wörtis, *Surf. Sci.* **259**, 314 (1991).
26. U. Breuer, H. Knauff, and H. P. Bonzel, *J. Vac. Sci. Tech.* **A8**, 2489 (1990).
27. A. Pavlovska, H. Steffen, and E. Bauer, *Surf. Sci.* **234**, 143 (1990).
28. A. W. D. van der Gon, H. M. Pinxteren, J. W. M. Frenken, and J. F. van der Veen, *Surf. Sci.* **244**, 250 (1991).
29. E. van de Riet, H. Derks, and W. Heiland, *Surf. Sci.* **234**, 53 (1990).
30. J. Sprösser, B. Salanon, and J. Lapujoulade, *Europhys. Lett.* **16**, 283 (1991).
31. W. Hetterich, C. Höfner, and W. Heiland, *Surf. Sci.* **251–252**, 731 (1991).
32. I. K. Robinson, E. Vlieg, and K. Kern, *Phys. Rev. Lett.* **63**, 2578 (1989).
33. U. Korte, Thesis, University of Osnabrück, unpublished (1992).
34. R. Vanselov, *Surf. Sci. Lett.* **279**, L213 (1991).
35. R. S. Williams, P. S. Wehner, J. Stöhr, and D. A. Shirley, *Phys. Rev. Lett.* **39**, 302 (1977).
36. H. Dürr, R. Schneider, and Th. Fauster, *Vacuum* **41**, 376 (1990).
37. M. Bienfait, *Surf. Sci.* **272**, 1 (1992).
38. S. Speller, M. Schleberger, and W. Heiland, *Surf. Sci.* **269–270**, 229 (1992).
39. M. Schleberger, S. Speller, C. Höfner, and W. Heiland, *Nucl. Instrum. Methods B* (1994) in press.
40. H. Niehus, W. Heiland, and E. Taglauer, *Surf. Sci. Repts.* **17**, 213 (1993).
41. A. Niehof and W. Heiland, *Nucl. Instrum.* **B48**, 306 (1990).
42. J. Lindhard, *K. Dan. Vidensk. Selsk. Mat. Fys. Medd.* **34**, 14 (1965).
43. M. Hou and M. Robinson, *Appl. Phys.* **17**, 371 (1978).

44. H. Derks, W. Hetterich, E. van de Riet, H. Niehus, and W. Heiland, *Nucl. Instrum. Methods* **B48**, 315 (1990).
45. J. Möller, K. J. Snowdon, W. Heiland, and H. Niehus, *Surf. Sci.* **178**, 475 (1986).
46. W. Hetterich, PhD Thesis, Univ. Osnabrück (1991).
47. T. Gritsch, D. Coulman, R. J. Behm, and G. Ertl, *Appl. Phys.* **A49**, 403 (1989),
48. R. L. Erickson and D. P. Smith, *Phys. Rev. Lett.* **34**, 297 (1975).
49. A. Zartner, E. Taglauer, and W. Heiland, *Phys. Rev. Lett.* **40**, 1259 (1978).
50. E. C. G. Stückelberg, *Helv. Phys. Acta* **5**, 369 (1932).
51. J. C. Tully, *Phys. Rev.* **B16**, 4324 (1977).
52. S. Schippers, S. Oelschig, W. Heiland, L. Folkerts, R. Morgenstern, P. Eeken, I. F. Urazgil'din, and A. Niehaus, *Surf. Sci.* **257**, 289 (1991).
53. C. Müller, Diplom-Arbeit, Univ. Osnabrück (1994) unpublished; C. Müller *et al.*, to be published.
54. H. D. Hagstrum, in *Inelastic Ion Surface Collisions*, eds. N. H. Tolk, J. C. Tully, and C. W. White (Academic, New York, 1977) p. 1.
55. D. J. O'Connor, Y. G. Shen, J. M. Wilson, and R. J. MacDonald, *Surf. Sci.* **197**, 277 (1988).
56. G. Engelmann, E. Taglauer, and D. P. Jackson, *Nucl. Instrum. Methods* **B13**, 240 (1986).
57. A. Richard and H. Eschenbacher, *Nucl. Instrum. Methods* **B2**, 444 (1989).
58. D. J. Godfrey and D. P. Woodruff, *Surf. Sci.* **105**, 438 (1981).
59. A. Närmann, R. Monreal, P. M. Echenique, F. Flores, W. Heiland, and S. Schubert, *Phys. Rev. Lett.* **64**, 1601 (1990).